Available online at www.sciencedirect.com

SciVerse ScienceDirect

Journal of the European Ceramic Society 32 (2012) 2333–2339

www.elsevier.com/locate/jeurceramsoc

A new simple synthesis and characterization of Sm-doped ceria and its homogeneous precursor $[Ce_{0.80}Sm_{0.20}(Ac)_3(Gly)]_n$

Tina Skalar [a,b], Jadran Maček [a,b], Amalija Golobič [a,*]

[a] Faculty of Chemistry and Chemical Technology, University of Ljubljana, Aškerčeva 5, 1000 Ljubljana, Slovenia
[b] Center of Excellence Low-Carbon Technologies (CO NOT), Hajdrihova 19, 1000 Ljubljana, Slovenia

Received 28 December 2011; received in revised form 3 February 2012; accepted 6 February 2012
Available online 3 March 2012

Abstract

A new method for the synthesis of $Ce_{0.80}Sm_{0.20}O_{1.90}$ is presented. A drying of a solution of ethylene glycol and stoichiometric amounts of the acetates $Ce(C_2H_3O_2)_3{\cdot}xH_2O$ and $Sm(C_2H_3O_2)_3{\cdot}xH_2O$ resulted in a highly crystalline product of $[Ce_{0.80}Sm_{0.20}(C_2H_3O_2)_3(C_2H_6O_2)]_n$, a new chained polymeric coordination compound. With the calcination of this precursor at 900 °C and sintering at 1150 °C, pure $Ce_{0.80}Sm_{0.20}O_{1.90}$, was obtained with the desired homogeneity and density. This paper reports elemental (CHN and ICP-MS) and single crystal X-ray structure analyses of the precursor $[Ce_{0.80}Sm_{0.20}(C_2H_3O_2)_3(C_2H_6O_2)]_n$. Its thermal decomposition to $Ce_{0.80}Sm_{0.20}O_{1.90}$ has been studied via HT-XRD and TG–DTA analysis. The structure and composition of $Ce_{0.80}Sm_{0.20}O_{1.90}$ was also confirmed by powder XRD (Rietveld refinement).

Keywords: Precursors-organic; Sintering; Fuel cells; X-ray methods; CeO_2; Samarium-doped ceria-SDC

1. Introduction

Samarium-doped ceria is a well-known material in modern ceramics because of its high oxygen ion conductivity.[1–4] This material can be used in high temperature fuel cells (SOFC) as an electrolyte. It was experimentally determined that the best ionic conductivity is achieved when the molar ratio of Ce:Sm is 80:20, and when the samarium and cerium are distributed homogeneously. Solid electrolytes should be highly dense for practical applications of SOFC(s) fulfilling the gas-tight requirements.[4,5] Most of the previous work is related to SDC, which was synthesized with the solid state method, gel precipitation method and combustion synthesis.[6–8] The dry syntheses (solid state) are simple, but they have some important disadvantages, including non-uniform particle distribution, high costs of milling, and contamination with impurities. The wet-chemical techniques allow more diversity in synthesis conditions and achieve desired particle size and shape on the nanometer level.[9,10] One of the most commonly used wet techniques is the Pechini method, which enables the preparation of homogeneous precursors on the nano-level, and the preparation of multicomponent metal oxides with very good homogeneity.[11,12] This method uses polyalcohol, citric acid (or nitric acid) and metal salts. The polyalcohol is thought to promote reticulation in the starting solution between polyalcohol and citric acid, called "esterification". The immobilization of metal cations in such polymers can prevent, or at least reduce, the cation mobility during the heat treatment, which preserves their good dispersion in the product.[4,5,13,14]

In this paper, we report a new, simplified modification of the Pechini method for the synthesis of $Ce_{0.80}Sm_{0.20}O_{1.90}$, in which there are only polyalcohol (ethylene glycol) and metal carboxylates (cerium acetate and samarium acetate) in the reaction mixture and no acid (instead of citric or nitric acid). Another unique factor is that the polymeric precursor of the final product is well defined, and chemically and structurally characterized. We also investigated the thermal decomposition of this precursor to the final product $Ce_{0.80}Sm_{0.20}O_{1.90}$, which has desired homogeneity and density.

2. Experimental

2.1. Synthesis of $[Ce_{0.80}Sm_{0.20}(C_2H_3O_2)_3(C_2H_6O_2)]_n$, *1*

17.68 g of cerium acetate $Ce(C_2H_3O_2)_3{\cdot}xH_2O$ (Sigma Aldrich, 99.9% pure, metals basis) and 3.65 g of

* Corresponding author. Tel.: +386 1 2419 104; fax: +386 1 2419 220.
E-mail address: amalija.golobic@fkkt.uni-lj.si (A. Golobič).

0955-2219/$ – see front matter © 2012 Elsevier Ltd. All rights reserved.
doi:10.1016/j.jeurceramsoc.2012.02.008

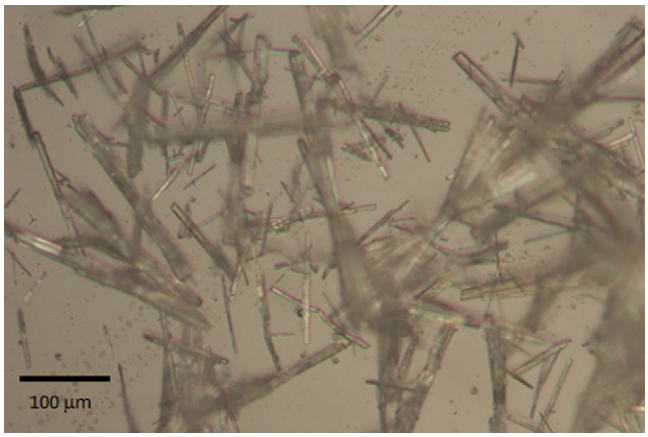

Fig. 1. Microscope image of single crystals of compound **1**.

$Sm(C_2H_3O_2)_3{\cdot}xH_2O$ (Sigma Aldrich 99.9% pure, metals basis) were dissolved in 150 ml of deionized water. The molar ratio in solution was 80:20 for Ce:Sm. After the dissolution of 100 ml of ethylene glycol ($C_2H_6O_2$, Sigma Aldrich, puriss. p.a. 99.5%) was added. The mixture was heated in a vacuum drier to 50 °C for 30 min; then the temperature was raised to 80 °C and held for 2.5 h. This precursor was then transferred to a conventional drier and left at the same temperature for three days. Light yellow needle-like single crystals were formed, which are presented in Fig. 1, and which were used for X-ray structure analysis. The microscope image was taken with a Leitz metallographic optical microscope.

2.2. Elemental analysis of compound *1*

Inductively coupled plasma atomic-emission spectrometry (ICP-AES) of compound **1** was carried out with a Perkin Elmer OPTIMA 3100RL spectrometer at the Institute of Metals and Technology, Ljubljana in order to obtain the content of cerium and samarium. Microanalysis of compound **1** for the determination of carbon and hydrogen content was performed with a Perkin-Elmer CHN Analyzer 2400 II at the Faculty of Chemistry and Chemical Technology, University of Ljubljana. $C_8H_{15}Ce_{0.80}O_8Sm_{0.20}$ requires: C, 0.252; H, 0.039; Ce, 0.294; Sm, 0.079; found C, 0.248; H, 0.035; Ce, 0.289; Sm, 0.071.

2.3. Calcination of $[Ce_{0.80}Sm_{0.20}(C_2H_3O_2)_3(C_2H_6O_2)]_n$ and sintering of $Ce_{0.80}Sm_{0.20}O_{1.90}$

Precursor **1** was calcinated at 900 °C for 1 h in a furnace to obtain mixed oxide $Ce_{0.80}Sm_{0.20}O_{1.90}$, designated as compound **2**. The obtained powder of samarium-doped ceria was milled with 3-mm diameter balls mounted on a planetary ball mill Fritsch Pulverisette 5. After milling, the powder was compacted with uniaxial pressing into cylindrical pellets 6 mm in diameter under a pressure of 410 MPa. The measurement of the sintering curve was performed with a Hesse Instruments heating microscope by heating the compressed powder of compound **2** to 1500 °C with a constant heating rate of 10 °C/min while taking pictures of a pellet. Fresh powder of compound **2**, again compacted to pellets as explained above, was sintered at 1150 °C for 1 h in air in a Carbolite 1600 STF 16/180 furnace. For microstructure determination, sintered tablets were polished (diamond paste 3 µm and 0.25 µm), thermally etched and analyzed with SEM (Zeiss Ultra Plus scanning electron microscope). The quantitative analysis of the microstructures was performed on digital images using image-analysis software Zeiss KS300 3.0.

The relative density of compacted SDC was determined from experimental and theoretical density. The theoretical density was calculated from the lattice parameters of compound **2**. The experimental density was determined from the height, diameter and mass of compressed and sintered pellets.

Compound **1** was also calcinated at 400, 600, 800 and 900 °C in order to determine the specific surface area of the obtained SDC. The specific surface area was determined by the Brunauer–Emmett–Teller (BET) method using a Micromeritics ASAP 2020 instrument.

The thermal decomposition of compound **1** was analyzed from room temperature to 800 °C in argon with a heat rate of 10 K/min using TG/DTA analysis with a Netzsch STA 449 F3 Jupiter apparatus.

2.4. Single-crystal structure analysis

Single crystal diffraction data for compound **1** have been collected on a Nonius Kappa CCD diffractometer at room temperature with Mo Kα radiation (0.71073 Å) and graphite monochromator. The data were processed using DENZO software.[15] The structure was solved by direct methods, using SIR97.[16] A full-matrix least-squares refinement on F2 was employed with anisotropic temperature displacement parameters for all non-hydrogen atoms. H atoms from hydroxy groups were found in a difference located from difference Fourier map. Only their isotropic displacement parameter was refined. The remaining H atoms were placed at calculated positions and treated as riding, with C—H = 0.97 and 0.96 Å and $U_{iso}(H) = 1.2U_{eq}(C)$ or $1.5U_{eq}(C)$ for CH_2 and CH_3, respectively. The metal ions, Ce^{III} and Sm^{III}, share the same site, so the identical fractional coordinates and displacement parameters for both atoms were applied. A trial refinement of their occupancy parameters, with their sum constrained to be 1, resulted into values 0.74(5) and =0.26(5) for Ce^{III} and Sm^{III}, respectively. Since the scattering power of both metal ions is similar, and since their occupancy is also correlated with their displacement parameters, it was more reliable to set the occupancy of the metal site as 0.8 and 0.2 for Ce^{III} and Sm^{III}, respectively, according to the results of an ICP-AES analysis, synthetic conditions and obtained molar Ce^{IV}:Sm^{III} ratio in the calcinated product, compound **2**. SHELXL97 software[17] was used for structure refinement and interpretation. Drawings of the structure were produced using ORTEPIII.[18] Details of the crystal data, data collection, and refinement parameters are listed in Table 1. Structural and other crystallographic data have also been deposited with the Cambridge Crystallographic Data Centre as supplementary publication number CCDC 859415. A copy of the data can be obtained, free of charge, by applying to CCDC, 12 Union

Table 1
Crystal data, data collection and refinement parameters for compound **1**.

Formula: $C_8H_{15}Ce_{0.80}O_8Sm_{0.20}$	$F(000) = 371.6$
$M_r = 381.37$	$Z = 2$
Triclinic	$D_x = 1.979\ Mg\ m^{-3}$
Space group: $P\bar{1}$, no. 2.	Mo $K\alpha$ radiation, $\lambda = 0.71073$ Å
$a = 8.7052(2)$ Å	Cell parameters from 2905 reflections
$b = 8.7646(3)$ Å	$\theta = 0.4–27.5°$
$c = 9.2738(3)$ Å	$\mu = 3.79\ mm^{-1}$
$\alpha = 81.249(2)°$	$T = 293$ K
$\beta = 67.782(2)°$	Yellow, needle, 0.30 mm × 0.02 mm × 0.02 mm
$\gamma = 78.711(2)°$	$V = 639.98\ (3)$ Å^3
Nonius Kappa CCD diffractometer	$\theta_{max} = 27.5°$
19405 measured reflections	$R_{int} = 0.038$
2912 independent reflections	2634 reflections with $I > 2\sigma(I)$
Refinement on F^2	2912 contributing reflections
$R[F^2 > 2\sigma(F^2)] = 0.022$	157 parameters
$wR(F^2) = 0.054$	9 constraints
$\Delta\rho_{max} = 1.03$ e Å^{-3} (close to metal ion)	$\Delta\rho_{min} = -0.54$ e Å^{-3}
$S = 1.11$	Extinction coefficient: 0.0060 (7)

Road, Cambridge, CB2 1EZ, UK (fax: +44 0 1223 336033 or deposit@ccdc.cam.ac.uk).

2.5. X-ray powder diffraction

All X-ray powder diffraction data were collected using a PANalytical X'Pert PRO MPD diffractometer with θ–2θ reflection geometry, primary side Johansson type monochromator and Cu$K\alpha_1$ ($\lambda = 1.54059$ Å) radiation. The HT-XRD of compound **1** was made from room temperature to 800 °C in vacuum with a heat rate of 10 K/min. The XRD patterns were acquired from 2Θ angles of 10–60° at 25, 110, 220, 400, 600 and 800 °C in steps of 0.034°.

The room temperature XRD pattern of compound **2** was acquired from 2Θ angles of 10–70° in steps of 0.034°. A Rietveld refinement using these data was performed using the *TOPAS*2.1, program suite.[19] The background was modeled by a third-order polynomial. Zero error, scale factor, lattice parameter a and one profile parameter were also refined. Atoms parameters were fixed, taken from the published structure of $Ce_{0.80}Sm_{0.20}O_{1.90}$.[20] The final match between observed and calculated profiles is shown in Fig. 2. The agreement factors were: 0.0965, 0.1204, 0.1125 and 1.07 for R_p, R_{wp}, R_{exp} and goodness of fit, respectively.

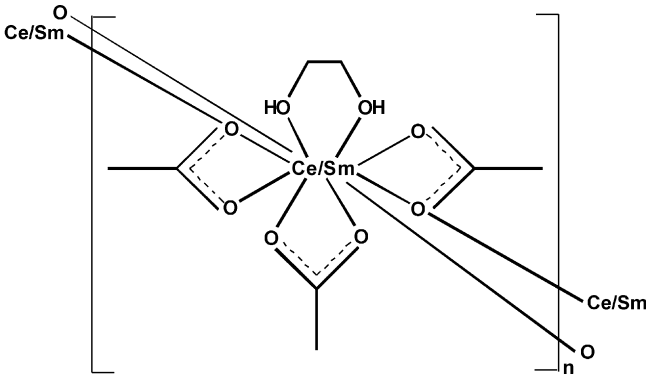

Fig. 3. Structural formula of one-dimensional compound **1**.

3. Results and discussion

A new coordination compound $[Ce_{0.80}Sm_{0.20}(C_2H_3O_2)_3(C_2H_6O_2)]_n$ was synthesized and structurally characterized, (**1**). With the calcination and sintering of this precursor at 1150 °C, samarium-doped ceria ($Ce_{0.80}Sm_{0.20}O_{1.90}$) was obtained (**2**) of proper density and with homogeneous distribution of samarium and cerium.

3.1. Crystal structure of $[Ce_{0.80}Sm_{0.20}(C_2H_3O_2)_3(C_2H_6O_2)]_n$, (1)

Compound **1** is an infinite one-dimensional coordination polymer with a structural formula shown in Fig. 3. The asymmetric unit consisting of one metal ion, one glycol molecule and three acetate ions is shown in Fig. 4. The central metal atom, which is 80% occupied by Ce^{III} and in 20% by Sm^{III}, is surrounded by ten O atoms at the vertices of an irregular hexadecahedron. Selected bond lengths are given in

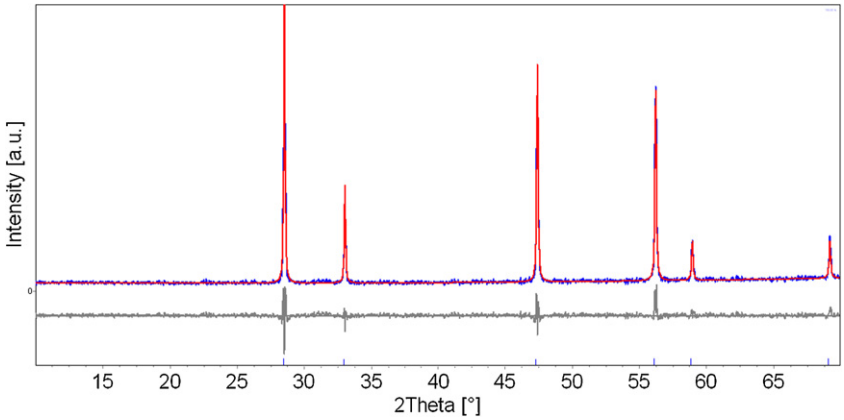

Fig. 2. Rietveld refinement for compound **2**: experimental (blue), calculated (red) and difference (gray) profiles. Vertical bars denote the position of reflections. (For interpretation of the references to colour in this figure legend, the reader is referred to the web version of the article.)

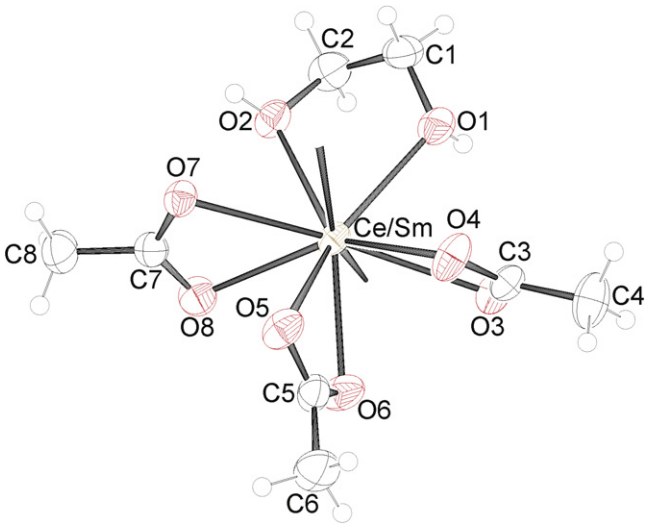

Fig. 4. A view of the asymmetric unit of compound **1**, showing the atom-numbering scheme. Displacement ellipsoids are drawn at 50% probability level and H atoms are shown as small spheres of arbitrary radii.

Table 2a
Selected geometric parameters (Å) in compound **1**.

Ce/Sm—O3^{i}	2.422 (2)	O2—C2	1.430 (4)
Ce/Sm—O7^{ii}	2.461 (2)	O3—C3	1.276 (4)
Ce/Sm—O4	2.527 (2)	O4—C3	1.246 (4)
Ce/Sm—O6	2.528 (2)	O5—C5	1.257 (4)
Ce/Sm—O8	2.570 (2)	O6—C5	1.262 (4)
Ce/Sm—O5	2.599 (2)	O7—C7	1.282 (4)
Ce/Sm—O1	2.618 (2)	O8—C7	1.241 (4)
Ce/Sm—O2	2.633 (2)	C1—C2	1.491 (5)
Ce/Sm—O7	2.651 (2)	C3—C4	1.494 (5)
Ce/Sm—O3	2.771 (2)	C5—C6	1.496 (5)
O1—C1	1.434 (4)	C7—C8	1.500 (5)

Symmetry codes: (i) $-x+1, -y+1, -z$; (ii) $-x+2, -y+1, -z$.

Table 2b
Hydrogen-bond geometry (Å,°) in compound **1**.

D—H···A	D—H	H···A	D···A	D—H···A
O1—H1···O6^{i}	0.8500	1.8400	2.686 (4)	170.00
O2—H2···O5^{ii}	0.8900	1.9100	2.779 (4)	165.00

Symmetry codes: (i) $-x+1, -y+1, -z$; (ii) $-x+2, -y+1, -z$.

Tables 2a and 2b. The glycol molecule and terminal acetate ligand are coordinated in bidenate chelate, *syn–syn* mode. The remaining two acetate ligands are coordinated in a tridentate mode: carboxyl group is (through both its O atoms) as an *syn–syn* chelate bonded to one central metal ion, and one of the O atoms from the carboxyl group is also simultaneously linked anti to another, symmetry-related (by a center of inversion) metal atom, forming a tridentate bridge. In this way, each Ce/Sm ion is bridged by four acetate bridges, and infinite chains running parallel *a* axis are formed (Fig. 5). The neighboring Ce/Sm coordination moieties within a chain are additionally connected by intra-molecular hydrogen bonds donated by O1 and O2 atoms from glycol hydroxyl groups and accepted by O6^{i} and O5^{ii}, respectively [symmetry codes: (i) $1-x$, $1-y$, $-z$ (ii) $2-x$, $1-y$, $-z$], from the non-bridging, chelate acetate group. The geometry of hydrogen bonds is presented in Table 2b.

Among the chains, van der Waals interactions predominate. The metal–metal separation within the chains is 4.4218(3) Å and 4.3340(3) Å. The smallest inter-chain metal–metal distance is 8.5187(3) Å.

The *catena*-poly[cerium(III)-tri-acetato-glycol] doped with samarium(III), compound **1**, is the first example of a coordination compound containing both glycol and acetate ligands. However, the comparison of coordination bond lengths is possible with known compounds of Ce^{III} or Sm^{III} containing coordinated acetate or glycol molecules. In similar complex bis((μ_2-acetato-O,*O*,*O*′)-tris(acetato-*O*,*O*′)-aqua-cerium(III)) and its samarium(III) isostructural analogue,[21] terminal bidentate chelate acetates are coordinated at distances in range 2.52–2.64 and 2.46–2.59 Å, respectively. The distances in Ce^{III} compound are slightly longer in comparison with Sm^{III} compound which is in agreement with the small difference in

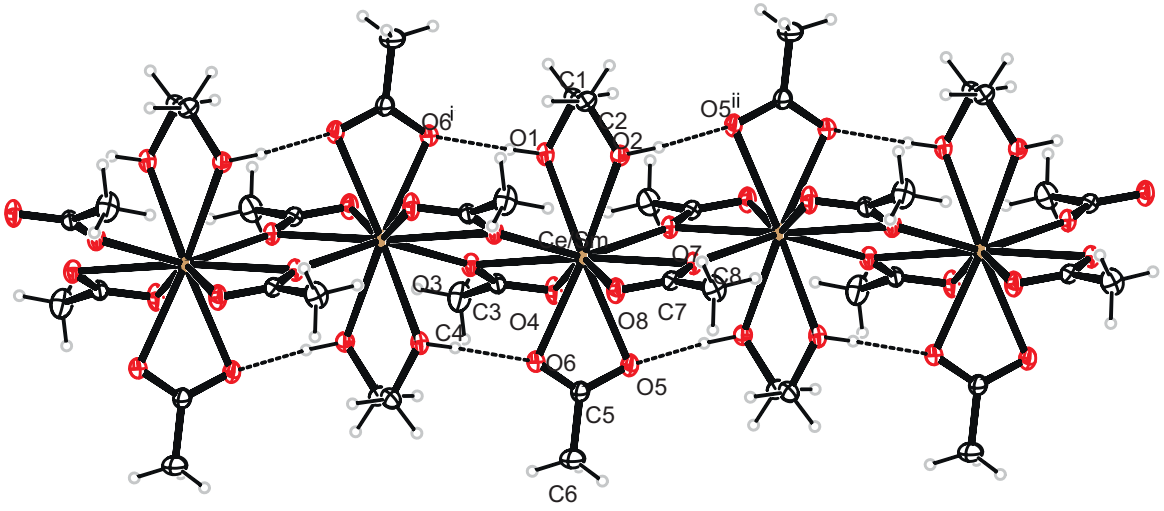

Fig. 5. The one-dimensional extended structure of compound **1** with displacement ellipsoids at 25% level. H atoms are shown as small spheres of arbitrary radii. Intramolecular O—H···O hydrogen bonds are shown as dashed lines. [symmetry codes: (i) $1-x$, $1-y$, $-z$, (ii) $2-x$, $1-y$, $-z$].

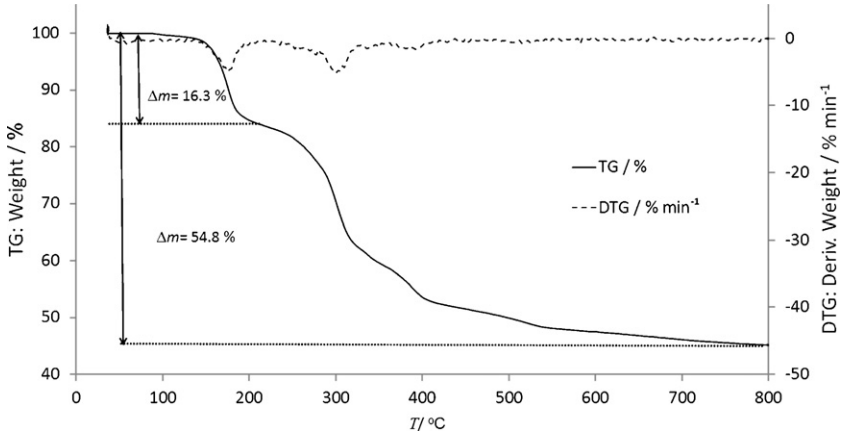

Fig. 6. Thermal decomposition of compound **1** in argon.

their ionic radia. In the mixed Ce^{III}, Sm^{III} compound **1**, terminal chelate acetate coordination bond distances are within the above ranges with 2.599(2) and 2.570(2) Å. There is also a good agreement among coordination bond lengths of tridentate bridging acetate ligands. In compound **1**, such distances for bridging O atom are 2.422(2) and 2.461(2) for *anti* and 2.651(2) and 2.771(2) Å for *syn* bonding. The bond length of the O atom with only one coordination bond is in between the values of bond distances of bridging O atom. The same is also observed in the abovementioned Ce^{III} and Sm^{III} acetate complex,[21] which are also ten-coordinated. The bond lengths within all carboxyl groups in compound **1** are similar as in both complexes reported in the abovementioned literature, and correspond to delocalized C–O bonds. In all three known structures of Sm^{III} or Ce^{III} with coordinated glycol molecule metal to O, bond lengths range in 2.45–2.60 Å[22,23] which is slightly shorter in comparison with 2.618(2) and 2.633(2) Å in compound **1**. This can be explained with the difference of coordination number, which is ten in compound **1** and seven in all three literature compounds.

3.2. Characterization of $Ce_{0.80}Sm_{0.20}O_{1.90}$, (2)

The structure of $Ce_{0.80}Sm_{0.20}O_{1.90}$, **2** was determined in 1954 as one in the serial compounds $Ce_{1-x}Sm_xO_{2-x/2}$ with $x = 0.1$, 0.2, 0.3 and 0.4.[20] It was shown that these compounds are isostructural with ceria (cerianite mineral, CeO_2) which has a cubic, fluorite structure ($a = 5.411$ Å).[24] Ce^{IV} and Sm^{III} are randomly distributed at the corners and the face centers of a cubic unit cell, and O^{2-} is at the centers of eight cubelets, in which the cell may be divided with an occupancy of 95%. The metal ions are eight and oxygen four coordinated. The lattice parameter *a* was shown to be slightly larger in comparison to cerianite: 5.423, 5.433, 5.443 and 5.450 Å for $x = 0.1$, 0.2, 0.3 and 0.4, respectively.[20] This is in accordance with the larger ionic radius of eight coordinated Sm^{III} (1.079 Å [25]) in comparison with eight coordinated Ce^{IV} (0.970 Å [25]). Rietveld refinement (Fig. 2) of powder diffraction pattern of compound **2** resulted to the lattice parameter *a* of 5.434(2) Å, which is additional confirmation that the molar ratio of Ce:Sm in compound **2** is 0.8:0.2.

3.3. Thermal decomposition of compound *1* to compound *2*

The TG and DTG curves of the thermal decomposition of compound **1** are presented in Fig. 6. The TG curve exhibits four thermal decomposition steps. At the first step between 150 °C and 180 °C, the mass loss was 16.3% and ethylene glycol was eliminated, which is in good agreement with the theoretical value (16.3%). It can be seen from the HT-XRD pattern measured at 220 °C that after leaving off glycol, the precursor, compound **1** had been already decomposed and the crystallization of the final product (SDC) had begun. Peaks in diffraction patterns (Fig. 7) at 220, 300, 400, 600 and 800 °C were assigned to $Ce_{0.80}Sm_{0.20}O_{1.90}$. The width of these peaks decreases with the temperature increase, due to the higher degree of crystallinity at higher temperatures. The thermal decomposition is completed at 800 °C. The measured mass loss for the overall decomposition ($\Delta m_{meas} = 54.8\%$) is also in good agreement with the calculated value ($\Delta m_{calc} = 54.7\%$).

3.4. Calcination, sintering and microstructure of compound *2*

The specific surface area of samples obtained by the calcination of compound **1** at 400, 600, 800 and 900 °C are presented in Table 3. When the compound **1** is calcinated at higher temperatures, the specific surface area of the powders reduces. For example after calcination at 400 °C, the BET surface area is 122 m^2/g and it sharply decreases to 24 m^2/g at 900 °C when the sintering process begins.

The appropriate temperature of sintering of compound **2**, 1150 °C was obtained by measurement of sintering curve, which

Table 3
The impact of the temperature of calcination on specific BET surface area.

$T_{calcination}$ (°C)	BET surface area (m^2/g)
400	122
600	72
800	65
900	24

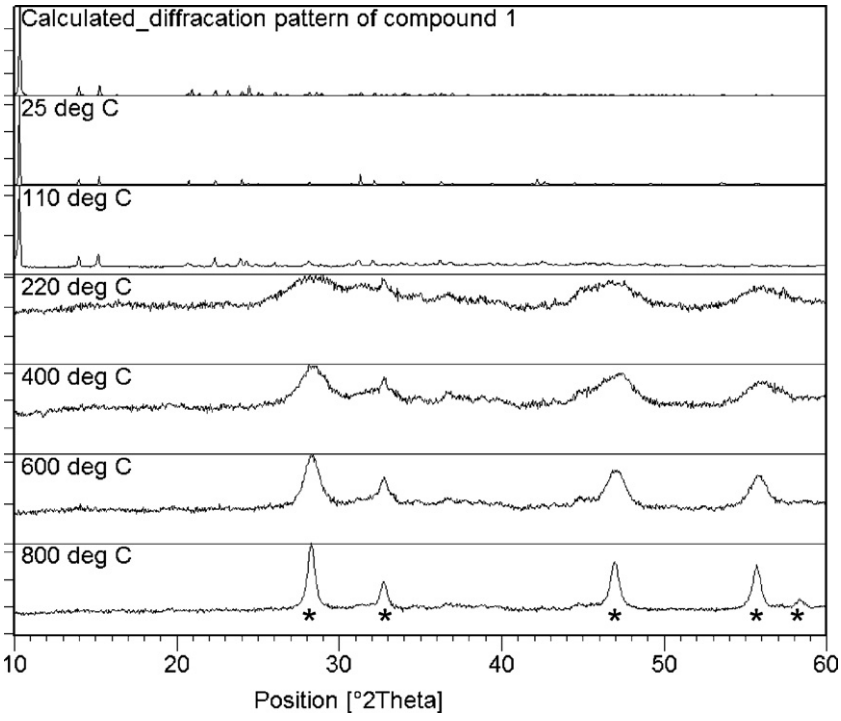

Fig. 7. HT-XRD for precursor **1** in vacuum. * the position of peaks of $Ce_{0.80}Sm_{0.20}O_{1.90}$.

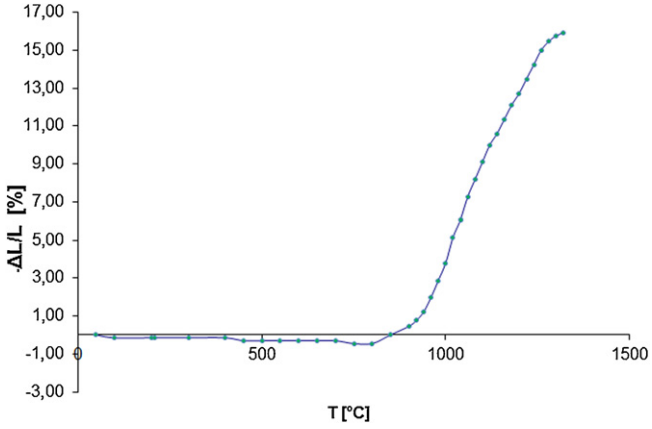

Fig. 8. Sintering curve for compound **2**.

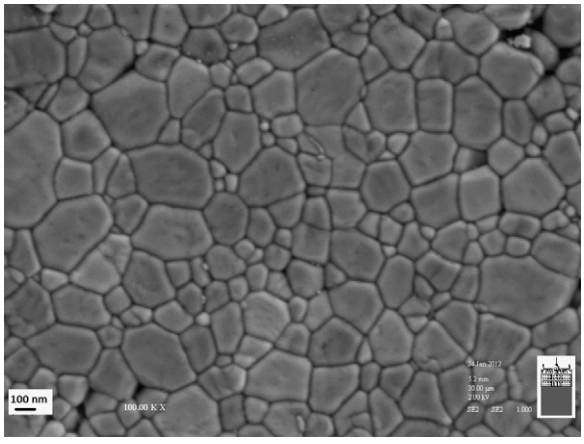

Fig. 9. SEM micrograph of calcinated pellet of compound **2** at 900 °C and sintered (densified) at 1150 °C.

is presented in Fig. 8. The microstructure of sintered compound **2** is shown in Fig. 9. The results of the quantitative microstructure analysis represent a diameter of the area-analogue circle (d) and intercept lengths in x and y direction (d_x and d_y). The mean values of d, d_x and d_y are 97.7, 108.5 and 108.9 nm, respectively. According to this, the grains are small. The relative density of the sintered pellets is 93%. On the basis of these results it can be concluded that the material is dense and homogeneous. Such SDC is suitable for electrolyte material where we need to prevent the mixing between oxidizing and reducing atmosphere.

4. Conclusion

This paper reports a new, simple synthesis of samarium-doped ceria, SDC, a well-known material for electrolytes in SOFC fuel cells. The final SDC product as well as its precursor (coordination polymer) are both well-defined crystalline single phases with known crystal structures including known chemical composition, confirming the desired Sm:Ce molar ratio and with homogeneous distribution of both metals. The final product after sintering is a material with appropriate density and particle size.

Acknowledgements

We are thankful for the financial contribution of the Ministry of Higher Education, Science and Technology of the Republic of Slovenia through grants P1-0175-103, P1-0A5-103, and Center of Excellence Low-Carbon Technologies (CO NOT).

References

1. Chen M, Kim BH, Xu Q, Nam OJ, Ko JH. Synthesis and performances of Ni-SDC cermets for IT-SOFC anode. *J Eur Ceram Soc* 2008;**28**:2947–53.

2. Chen M, Kim BH, Xu Q, Ahn BK, Kang WJ, Huang DP. Synthesis and electrical properties of Ce(0.8)Sm(0.2)O(1.9) ceramics for IT-SOFC electrolytes by urea-combustion technique. *Ceram Int* 2009;**35**:1335–43.
3. Wright J, Virkar A. Conductivity of porous Sm(2)O(3)-doped CeO(2) as a function of temperature and oxygen partial pressure. *J Power Sources* 2011;**196**:6118–24.
4. Li JG, Ikegami T, Mori T. Low temperature processing of dense samarium-doped CeO_2 ceramics: sintering and grain growth behaviors. *Acta Mater* 2004;**52**:2221–8.
5. Yoshida H, Deguchi H, Kawano M, Hashino K, Inagaki T, Ijichi H, et al. Study on pyrolysing behavior of NiO–SDC composite particles prepared by spray pyrolysis technique. *Solid State Ionics* 2007;**178**:5–6, 399–405.
6. Dong Li W. Combustion synthesis of ceramic nanoparticles for solid oxide fuel cells. *Asia–Pac J Chem Eng* 2010;**5**:593–8.
7. Chen M, Kim BH, Xu Q, Ahn BK, Kang WJ, Huang D. Synthesis and electrical properties of Ce(0.8)Sm(0.2)O(1.9) ceramics for IT-SOFC electrolytes by urea-combustion technique. *Ceram Int* 2009;**35**:1335–43.
8. Ji Y, Liu J, He TM, Cong LG, Su WH. Electrolyte and electrode materials of inter-medium-temperature SOFC prepared by glycine-nitrate process. *Chem J Chinese U* 2002;**23**:1227–30.
9. Cezar Grzebielucka E, Scoton Antonio Chinelatto A, Mazurek Tebcherani S, Luiz Chinelatto A. Synthesis and sintering of Y_2O_3-doped ZrO_2 powders using two Pechini-type gel routes. Short communication. *Ceram Int* 2010;**36**:1737–42.
10. Cheng JG, Deng LP, Xiong ET, Shi P. NiO-SDC powder of solid oxide fuel cell anode applications by buffer solution method. *Key Eng Mat* 2007;**440**:336–8.
11. Pechini MP, Adams N. US Patent 33,30,697; 1967.
12. Ertl G, Knoezinger H, Schueth F, Weitkamp J, editors. *Handbook of heterogeneous catalysis*. 2nd ed. Weinheim: Wiley-VCH; 2008. p. 295–318.
13. Razpotnik T, Maček J. Synthesis of nickel oxide/zirconia powders via a modified Pechini method. *J Eur Ceram Soc* 2007;**27**:1405–10.
14. Gaudon M, Laberty-Robert C, Ansart F, Stevens P, Rousset A. Preparation and characterization of $La_{1-x}Sr_xMnO_3$ + delta ($0 <= x <= 0.6$) powder by sol-gel processing. *Solid State Sci* 2002;**4**:125–33.
15. Otwinowski Z, Minor W. In: Carter Jr CW, Sweet RM, editors. *Methods in enzymology, Vol. 276, Macromolecular crystallography, Part A*. New York: Academic Press; 1997. p. 307–26.
16. Altomare A, Burla MC, Camalli M, Cascarano G, Giacovazzo C, Guagliardi A, et al. SIR97: a new tool for crystal structure determination and refinement. *J Appl Cryst* 1999;**32**:115–9.
17. Sheldrick GM. A short history of SHELX. *Acta Cryst A* 2008;**64**:112–22.
18. Farrugia LJ. ORTEP-3 for Windows—a version of ORTEP-III with a Graphical User Interface (GUI). *J Appl Cryst* 1997;**30**:565.
19. Topas2.1: General Profile. *Structure analysis software for powder diffraction data, Bruker AXS*. Karlsruhe: Germany; 2003.
20. Brauer G, Gradinger H. Ueber heterotype Mischphasen bei Seltenerdoxyden. *Z Anorg Allg Chem* 1954;**276**:209–26.
21. Sawase H, Koizumi Y, Suzuki Y, Shimoi M, Ouchi A. The bridging tridentate-type carboxilato ligand in isomorphous guanidinium di(mu-acetato)bis(triacetatoaqualanthanoidates(III)), $[(NH_2)_3C]_2$-$[M_2(CH_3CO_2)_8(H_2O)_2]$, (M = La, Ce, Pr, Nd and Sm). *B Chem Soc Jpn* 1984;**57**(10):2730–7.
22. Wang Y, Li X, Wang T, Song Y, You X. Slow relaxation processes and single-ion magnetic behaviors in dysprosium-containing complexes. *Inorg Chem* 2010;**49**:969–76.
23. Liu Y, Tang M, Lii K. Rare earth metal squarates incorporating ethylene glycol ligand with a three-dimensional framework structure: $RE(C_4O_4)_{1.5}(C_2H_6O_2)$ (RE = Y, La–Nd, Sm–Lu). *Dalton Trans* 2009:9781–6.
24. Harwood MG. Variation in density and colour of cerium oxide. *Nature* 1949;**164**:787.
25. Shannon RD. Revised effective ionic radii and systematic studies of interatomic distances in halides and chalcogenides. *Acta Cryst* 1976;**A32**:751–67.